Weak localization effect in the strongly ferromagnetic Kondo compound $UCo_{0.5}Sb_2$

V. H. Tran, R. Troć, Z. Bukowski, D. Badurski, and C. Sułkowski
W. Trzebiatowski Institute of Low Temperature and Structure Research, Polish Academy of Sciences, P.O. Box 1410, 50-950 Wrocław, Poland

(Received 3 June 2004; revised manuscript received 13 September 2004; published 30 March 2005)

Experimental results of the magnetization (M), specific heat (C_p), electrical resistivity (ρ), magnetoresistance (MR), and thermoelectric power (S) are presented for single crystals of the tetragonal $UCo_{0.5}Sb_2$ compound. Anomalies in the *M(T)*, $[C_p(T)]$, *ρ(T)*, *S(T)* dependencies have allowed us to establish that $UCo_{0.5}Sb_2$ undergoes a long-range ferromagnetic ordering at $T_C = 64.5(2)$ K. The temperature dependence of the magnetization measured fairly far below T_C might be explained by considering both types of magnetic excitations: i.e., the spin-wave- and Stoner-type excitations. The *M(T)* dependence is well represented by the relation $1 - M(T)/M_s = BT^{3/2} + B_1 T^{3/2}\exp(-\Delta/T)$ with the determined spin-wave stiffness constant $D \sim 100$ meV Å^2 and a Stoner gap $\Delta = 69(2)$ K. The behavior of the electrical resistivity below about $T_C/2$ is discussed in terms of the electron scattering on magnons with a dispersion relation $E_q = \Delta + Dq^2$ and the two-dimensional weak localization effect described by a $-\ln T$ dependence. Negative magnetoresistance is observed over a wide range of temperatures below 150 K. The relative large field and temperature changes in the transverse MR around T_C are thought to be due to the ferromagnetic order or/and damped critical fluctuations by the applied fields. Below 40 K the magnetoresistance behavior may be understood on the basis of the predominant elastic scattering predicted for two-dimensional systems with the weak localization effect. The thermoelectric power data indicate $UCo_{0.5}Sb_2$ to be a *p*-type material with a moderate S value of ~ 25 μV/K at room temperature. The $T^{3/2}$ dependence observed in the *S(T)* curves for $T \leqslant 30$ K is consistent with the electron-magnon scattering process. The high anisotropy and temperature dependence of the *S(T)* curves may be explained by adopting a phenomenological model for a Kondo lattice.

DOI: 10.1103/PhysRevB.71.094428 PACS number(s): 72.15.Rn, 73.20.Mf, 75.30.Ds

I. INTRODUCTION

It is accepted nowadays that the magnetic behavior of uranium intermetallic compounds is intimately associated with the so-called dual nature of the $5f$ electrons of the uranium atoms.[1,2] In this concept, part of the $5f$ electrons behaves itinerant whereas the remaining electrons behave localized. The former hybridize with the conduction and/or valence electron states of ligands and form energy bands while the latter form multiplets to reduce the local Coulomb repulsion. Correspondingly, we expect a mass enhancement of the delocalized quasiparticles and the formation of the local moments as well. However, physical properties of compounds depend not only on the interplay between these two phenomena but also on those involved in the interatomic exchange interactions throughout the Ruderman-Kittel-Kasuya-Yosida (RKKY) or superexchange mechanisms. These latter kinds of interactions are often accompanied by an unusual high anisotropy, much affecting the magnetic and electronic transport properties.

The existence of intermetallic compounds $UTSb_2$ (T=Ru, Fe, Co, Ni, Pd, Cu, Ag, and Au) was reported by Kaczorowski *et al.*[3] and Brylak *et al.*[4] The first authors have also measured magnetic susceptibility, electrical resistivity, neutron powder diffraction, and Mossbauer spectra. They have been found to pass an interesting evolution in the magnetic properties, ranging from a paramagnetic ($UFeSb_2$) through an antiferromagnetic ($UTSb_2$, T=Ru, Ni, and Pd) to a ferromagnetic behavior (T=Cu, Ag, and Au).[3] This evolution clearly demonstrates the decisive influence of the U$5f$-Td hybridization effect connecting with the number of the d electrons involved. Moreover, due to the interplay of crystal field and Kondo-like effects as well as the f-p mixing mechanism, the series of $UTSb_2$ compounds exhibits both a reduction of magnetic uranium moments (more of the itinerant character) and a strong magnetocrystalline anisotropy (a great deal of the localized character),[3] resembling the behavior being understood in a framework of the $5f$-electron dualism aforementioned.

Since investigations of the $UTSb_2$ compounds have been performed so far only on polycrystalline samples and hence information on their anisotropy of the physical properties is limited, we have prepared single crystals of all the ternaries $UTSb_2$ in order to shed more light on the unusual dual nature of the $5f$ electrons. A paper on characterization of single crystals and preliminary measurements of magnetization of $UCo_{0.5}Sb_2$ was published elsewhere.[5]

In this paper, we expanded investigation on magnetization, specific heat, electrical resistivity, magnetoresistance, and thermoelectric power on single crystals of $UCo_{0.5}Sb_2$. We report that this compound orders ferromagnetically below 64.5 K and shows a huge magnetocrystalline anisotropy in all the studied magnetic and electronic transport properties. Moreover, we have also established that the spin-wave theory is quite suitable for the interpretation of the magnetic and electronic transport properties of this compound. One of the most unusual properties found in $UCo_{0.5}Sb_2$ is its behavior being consistent with the so-called two-dimensional weak localization (2DWL) effect.

II. EXPERIMENT

Single crystals of $UCo_{0.5}Sb_2$ have been grown from molten Sb by a flux method similar to that applied earlier for the compound $UNi_{0.5}Sb_2$.[6] Uranium (purity 99.98%), cobalt and antimony (purity 99.99%) were weighed in the atomic ratio of 1:1:12 and placed in an alumina crucible. Single crystals of a typical size $3\times5\times1$ mm^3 were obtained after slow cooling the constituent bath from 1150 to 600 °C. For purpose of homogenization, crystals wrapped in Ta foil were sealed in an evacuated silica tube and annealed at 850 °C for two weeks. Purity of such obtained crystals were checked using an optical microscope and a scanning electron microscope (SEM) Phillipps 515, powder and single-crystal x-ray diffraction (XRD). $UCo_{0.5}Sb_2$ is found to crystallize in a tetragonal $HfCuSi_2$-type structure, space group $P4/nmm$ with $Z=2$ formula units per cell, and the lattice parameters $a=428.6(1)$ and $c=883.2(2)$ pm and atomic position parameters $z_U=0.2755(2)$ and $z_{Sb}=0.6381(2)$.[5] We note that the energy dispersive x-ray analysis (EDX) and single crystal x-ray-diffraction analysis of the selected crystals indicated a significant deviation from the 1:1:2 stoichiometry. The chemical composition was around $UCo_{0.5}Sb_2$, as it was found earlier in the case of $UNi_{0.5}Sb_2$.[6]

The magnetization measurements were performed by a superconducting quantum interference device (Quantum Design) in fields up to 5 T and in the temperature range 1.7–300 K. Electrical resistivity was measured in the temperature range 1.3–300 K, using a four probe dc technique with a current of 30 mA. Electrical contacts were made with Cu wire, connected with silver conductive paint. Transverse magnetoresistance data were collected in two different ways: isofield data in $B=\mu_0H=8$ T on zero-field cooled (ZFC) samples and isothermal data taken at several selected temperatures between 4–100 K and in magnetic fields up to 8 T. Thermoelectric power was measured in the temperature range 4–300 K using a steady method.

III. RESULTS

A. Magnetization

Figure 1 shows the magnetization in magnetic fields applied up to 5 T parallel $M_\parallel$ and perpendicular $M_\perp$ to the c axis. The magnetization data were taken on samples cooled in zero field. $M_\parallel$ at 2 K and at a field of 5 T tends to saturation, reaching a value of $\sim1.1\mu_B$. It should be noted that at this temperature M vs μ_0H shows a jump due to effect of narrow walls of domains at a large critical value μ_0H_c of about 1.5 T. The value of H_c shifts down to lower values with increasing temperature. The jump in the magnetization $M(H)$ curves is no longer observed at temperatures above 40 K. On the other hand, $M_\perp$ is almost linear in μ_0H, exhibiting very small values. This fact reflects a huge magnetocrystalline anisotropy existing in this compound. It is also clear from the figure that the observed magnetization at low temperatures is strongly reduced to a rather small value compared to the moment of $3.62\mu_B$ of the U^{3+} free ion. At temperatures above T_C, we recognize that there are still ferromagnetic correlations manifesting with the curvature of the magnetization. These correlations vanish for temperatures above 150 K, where the magnetization starts to be linear in the applied field.

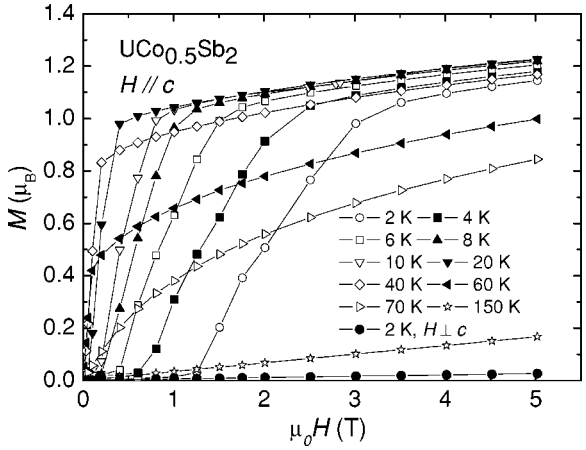

FIG. 1. Magnetization in magnetic fields applied parallel to the c axis at selected temperatures. The data for H perpendicular to the c axis at 2 K (closed circles) is also shown.

Figure 2 shows the temperature dependence of magnetization of a $UCo_{0.5}Sb_2$ single crystal taken at three magnetic field strengths applied along the c axis. The single-crystalline sample was cooled in the presence of the field. In order to interpret the magnetization data we first based on the spin-wave theory.[7,8] According to this theory, the expression for the magnetization as a function of temperature is

$$1-\frac{M(T)}{M_s}=BT^{3/2}+B_1T^{5/2}+B_2T^{7/2}\cdots, \qquad (1)$$

where the coefficient B is related to the spin-wave stiffness constant D, through $B=2.612[g\mu_B/M(0)](k_B/4\pi D)^{3/2}$ (g is the Landé factor, μ_B is the Bohr magneton, and k_B is the Boltzmann constant). The constants B_1 and B_2 involve both the spin-wave stiffness and average mean-square range of the exchange interaction. It turns out that a fit made first with a

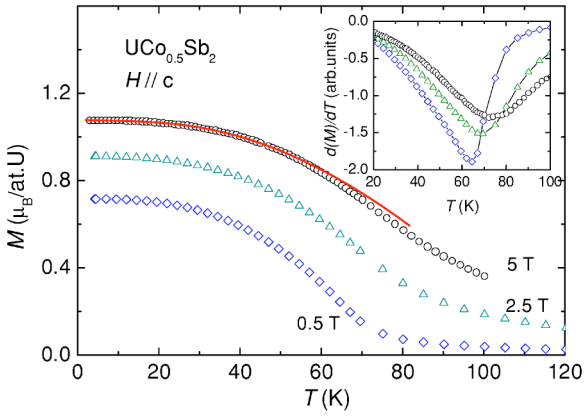

FIG. 2. Temperature dependence of the magnetization measured in fields: 0.5, 2.5, and 5 T applied parallel to the c axis. The solid line is a fit to the experimental 5-T data. The temperature derivatives of the magnetization as a function of temperature are shown in the inset.

simple $T^{3/2}$ law does not converge. Inclusion of higher spin-wave terms, such as $T^{5/2}$ or $T^{7/2}$, has not improved the fitting as well. Therefore, the observed deviation requires one to consider the possibility of other contributions to the total magnetization, such as, for instance, the magnon-magnon interaction or a Stoner excitation. Finally, we have gotten a remarkably good fit by taking into account both the free magnon and Stoner excitation contributions, which means the treating $UCo_{0.5}Sb_2$ as a strong ferromagnet. In fact, the magnetization data below 35 K were followed well by the relation

$$1 - \frac{M(T)}{M_s} = BT^{3/2} + B_1 T^{3/2}\exp(-\Delta/T). \qquad (2)$$

Here, Δ is the characteristic Stoner gap between the top of the full subband and the Fermi energy. It should be noted that the expression for magnetization [Eq. (2)] was derived by Thompson *et al.*[9] and was applied for a number of strong ferromagnets, e.g., for the crystalline nickel[10] and some amorphous ferromagnetic materials such as $Fe_xNi_{80-x}B_{18}Si_{20}$ and $Fe_{80}B_{20}$.[11] The fit of Eq. (2) to our experimental data is shown as the solid line in Fig. 2 with the following parameters: $\Delta = 69(2)$ *K*, $B = 8 \times 10^{-5}\ K^{-3/2}$, and $B_1 = 1.1 \times 10^{-3}\ K^{-3/2}$. Taking $V = 84\ A^3$ and $g = 0.667$ for U^{3+} or $g = 0.8$ for U^{4+} we have calculated the value of the spin-wave stiffness coefficient $D = 97.5$ or 110 meV Å^2 for respective U^{3+} and U^{4+} ions. Hence, the resulting ratio D/k_BT_C, characterized by the nearest-neighbor exchange interaction strength, amounts to 17.5–19.8 Å^2 which is a similar order of magnitude to that found in an itinerant electron ferromagnet, MnSi (19.3 Å^2),[12] but considerably smaller than that in UFe_2 (31 Å^2).[13]

From the temperature dependence of the magnetization measured at low field we evaluated the Curie temperature by taking T_C as a minimum in the temperature derivative of the $M(T)$ curve. For $UCo_{0.5}Sb_2$ a minimum of dM/dT taken at 0.5 T was found to be 64.8 K (inset of Fig. 2). Typically for a ferromagnet, the application of a magnetic field shifts the inflection point of the $M(T)$ curves to higher values, e.g., from 64.8 K at 0.5 T to 73 K at 5 T. The Curie temperature of $UCo_{0.5}Sb_2$ may be determined in a more precise manner with the help of an Arrott plot M^2 vs H/M as shown in Fig. 3. Clearly, the slope of the M^2 vs H/M curves for temperatures near T_C is positive. Therefore, we may analyze the data assuming the ferromagnetic transition in $UCo_{0.5}Sb_2$ to be second-order. From this figure, one can see that the M^2 vs H/M curves are basically linear in high fields and their intercept with the vertical and horizontal axes correspond to the square of the spontaneous magnetization M_s and to the inverse of the zero-field susceptibility $\chi(0)$ of the compound, respectively. In Fig. 4 M_s and $\chi(0)$ are plotted as a function of the reduced temperature $t = |(T - T_C)|/T_C$. Near a second-order phase transition both M_s and $\chi(0)$ should show power law dependence on t with critical exponents β and γ, respectively. For the investigated single crystal of $UCo_{0.5}Sb_2$ a least squares analysis yields $T_C = 64.4(1)$ K and $\beta = 0.34(2)$ from the M_s vs t^β dependence [Fig. 4(a)] and $T_C = 64.6(1)$ K and $\gamma = 1.13(2)$ from the $\chi(0)$ vs $t^{-\gamma}$ dependence [Fig. 4(b)]. The

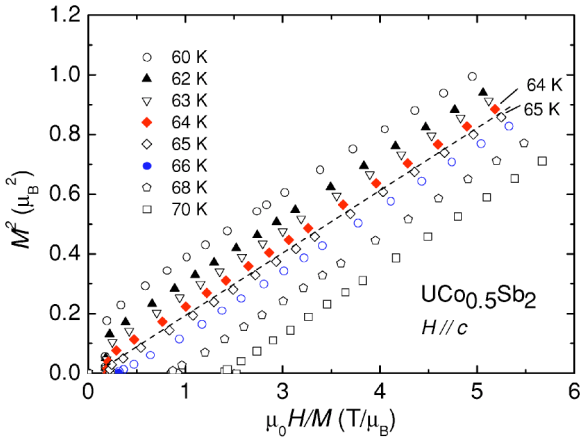

FIG. 3. Arrot plots of the magnetization isotherms for temperatures near T_C. The dashed line indicating T_C is a guide for the eye.

obtained critical exponents differ from those of the mean-field theory ($\beta = 0.5$ and $\gamma = 1$), but are comparable to those deduced from the classical Heisenberg model ($\beta = 0.38$ and $\gamma = 1.375$).[14]

The temperature dependences of the magnetic susceptibility $\chi(T) = M(T)/\mu_0 H$ with $\mu_0 H$, measured along the *c* axis and in the *ab* plane, were presented in our previous paper.[5] As was found, the high-temperature susceptibility follows the Curie-Weiss law, yielding the effective magnetic moment μ_{eff} of approximately $3\mu_B$/at. U for both these configurations.[5] This finding strongly points out that the effective magnetic uranium moment in $UCo_{0.5}Sb_2$ is high and close to the theoretical free ion values of 3.62 and 3.58 μ_B for U^{3+} and U^{4+}, respectively. This reflects rather a local behavior of the uranium ions in this ternary antimonide. We observe the huge magnetocrystalline anisotropy in $UCo_{0.5}Sb_2$, reflected by a large difference in the paramagnetic Curie temperatures $\Delta\Theta = \Theta_{\parallel} - \Theta_{\perp} = 255$ K.

B. Specific heat

In Fig. 5 we show the specific heat divided by temperature C_p/T below 250 K. The sharp peak near 64.5 K is con-

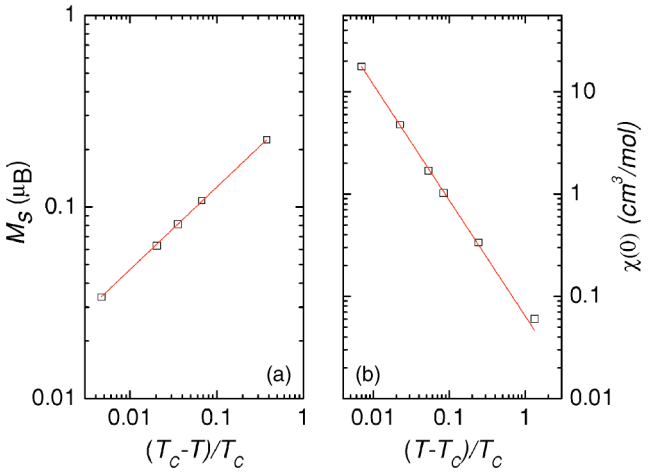

FIG. 4. M_s and $\chi(0)$ (from intercepts in Fig. 2) vs the reduced temperature. The solid lines are the fits.

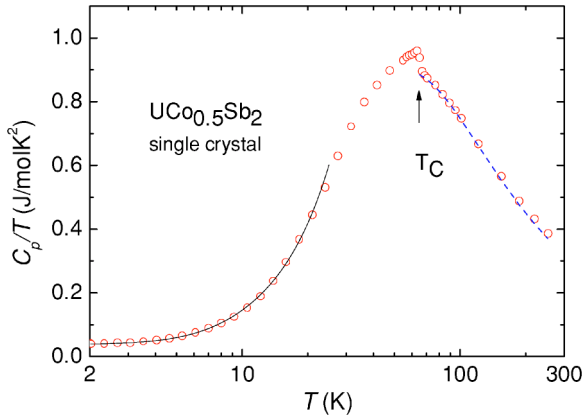

FIG. 5. Semilogarithmic scale temperature dependence of the specific heat divided by temperature. The dashed line presents the Debye function with $\Theta_D = 215$ K. The solid line is a fit.

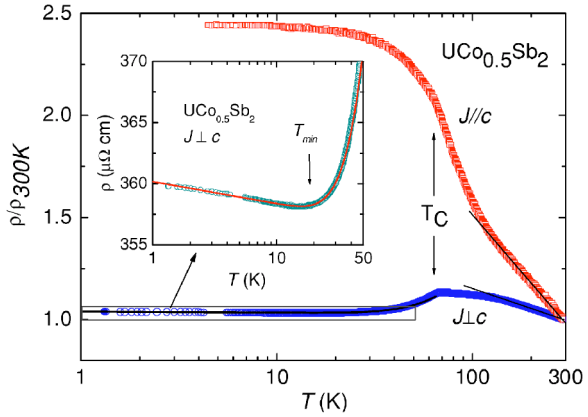

FIG. 6. Temperature dependence of the electrical resistivity for J flowing perpendicular and parallel to the c axis of the sample in semilogarithmic scale. The solid and dashed lines are the fits to the experimental data. The inset shows the low-temperature part of the resistivity with $J \perp c$ axis together with the fit.

sistent with the ferromagnetic transition implied by the magnetic measurements. The specific-heat data in the temperature range 2–8 K may be analyzed as a sum of two different contributions: the electronic $C_{\rm el}$ and phonon $C_{\rm ph}$ contributions, which are assumed to be dependent on temperature as $C_{\rm el}(T) = \gamma T$ and $C_{\rm ph}(T) = \beta T^3$, respectively. From the fit of the experimental data we obtained $\gamma = 35.6(2)$ mJ/mol K^2 and $\beta = 1.03(5)$ mJ/mol K^4. The latter value allows us to determine the Debye temperature through the relation

$$\beta = \frac{12}{5} R \pi^4 \left(\frac{T}{\Theta_D} \right)^3. \tag{3}$$

Using the above equation we estimated $\Theta_D = 211$ K. This value is very close to $\Theta_D = 215$ K, for which the Debye function $C_{\rm ph} = (9 N_A k_B T^3/\Theta_D^3) \int_0^{\Theta_D/T} [x^4 e^4/(e^x - 1)^2] dx$ reproduces quite well the experimental data for temperatures above T_C (dashed line in Fig. 5).

Based on the model developed by Andersen and Smith for the electron-magnon scatterring in ferromagnets,[18] where the magnetic contribution to the total specific heat is given as $C_{\rm mag}(T) = \sigma T^{0.5} \exp(-\Delta/k_B T)$, where Δ is an energy gap in the magnon spectrum, we have analyzed our data between 2–20 K (solid line in Fig. 5). Assuming $C_{\rm ph}(T) = \beta T^3$ for this temperature range we obtained $\gamma = 36(1)$ mJ/mol K^2, $\beta = 0.78(5)$ mJ/mol K^4, $\sigma = 490$ J/mol $K^{1.5}$, and $\Delta = 50(1)$ K in the fitting of the equation $C_p = C_{\rm ph} + C_{\rm el} + C_{\rm mag}$ to the experimental data. It is recommended that the magnetic contribution obtained via subtracting the phonon and electronic contributions from the total specific heat should be examined separately. However, for $UCo_{0.5}Sb_2$ there is still a lack of a suitable non-f-electron reference compound. Therefore, the absolute values of the fitting parameters should be taken with some caution.

C. Electrical resistivity

Figure 6 displays the temperature dependence of the electrical resistivity from 1.3 to 300 K for the electric current $J \perp c$ axis and from 4 to 300 K for the electric current $J \| c$ axis. As seen, the linear temperature dependence, being characteristic of the phonon resistivity at high temperatures, is not observed here. Instead, the resistivity shows a $-\ln T$ dependence with decreasing temperature. This is indicative of a considerable contribution originating from the Kondo-type scattering of the conduction electrons on the localized uranium moments. Taking into account the impurity scattering and spin-disorder contributions, the experimental data between 160–300 K can be perfectly fitted with the equation

$$\rho(T) = \rho_{0,HT} + C \ln T, \tag{4}$$

where $C \ln T$ is the Kondo resistivity and $\rho_{0,HT}$ denotes the temperature-independent resistivity, containing both the residual and spin-disorder contributions. The fit of the experimental data for $J \perp c$ (dashed line) gives $C = -48.0(5)$ $\mu\Omega$ cm K^{-1} and $\rho_{0,\rm HT} = 623\,(1)\,\mu\Omega$ cm. We are restrained to give the absolute values of the resistivity measured with $J \| c$ axis because of the uncertainty about the sample dimension in the measured configuration.

A clear evidence of the anisotropy appears at low temperature. For $J \| c$ the resistivity continuously increases and saturates at low temperatures. In contrast to $J \| c$, $J \perp c$ below 160 K starts to deviate from the Kondo-type behavior. First, it goes through a local maximum and then drops rapidly at $T_C = 65$ K. Unexpectedly, at about 20 K $\rho_\perp(T)$ exhibits a shallow minimum (see the inset of Fig. 6) and a logarithmic dependence with temperature below this minimum. The onset of the magnetic ordering is revealed by a peak in the temperature derivative of the resistivity, typical of a Fisher-Langer-type anomaly,[15] owing to the loss of spin disorder scattering just below the Curie point. Hence, the Curie temperature of 65 K could be determined exactly by the peak in the $d\rho(T)/dT$ curve (not shown here).

In conventional ferromagnets, with single-magnon type scattering, the low-temperature magnetic resistivity $\rho_{\rm mag}$ is described by a T^2 dependence.[16,17] For $UCo_{0.5}Sb_2$, attempts of fitting this power law to the experimental data have failed. However, a convergent fit could be achieved if one assumes

the existence of a gap Δ in the magnon spectrum. According to the model of Anderson and Smith,[18] describing electron scattering by magnon with a dispersion $E_q=\Delta+Dq^2$, the magnetic resistivity is as follows:

$$\rho_{\mathrm{mag}} = A\frac{T\Delta}{k_B}\exp(-\Delta/k_BT) \times\left(1+2\frac{T}{\Delta/k_B}+1/2\,\exp(-\Delta/k_BT)+\cdots\right). \quad (5)$$

Utilizing this equation we could obtain a satisfied fit but only in the temperature range 20–50 K. This is due to a subtle increase in the resistivity below 20 K mentioned above. A similar upward increase in the resistivity has been observed in a number of uranium alloys, for instance, $U_{1-x}Th_xRu_2Si_2$,[19] U_2Ni_2In,[20] and $U_2(Ni_{1-x}Pt_x)_2In$,[21] as well as in cerium alloys, such as $La_{1-x}Ce_xCu_6$,[22] $La_{1-x}Ce_xPd_3$,[23] and $Ce_{2-x}R_xNi_3Si_5$ (R=Y, Gd and x=0.1).[24] For all these alloys, a Kondo-hole scattering mechanism[25–27] was proposed. One could add that some uranium and thorium alloys displaying a structural disorder, such as UAsSe (Ref. 28) and ThAsSe (Ref. 29) were also found to exhibit an upturn in the resistivity at low temperatures. This behavior was attributed to the so-called nonmagnetic Kondo effect, based on the two-level system Kondo model.[30] In fact, the resistivity data of $UCo_{0.5}Sb_2$ at low temperature is very well described by the $-\ln T$ dependence (see Fig. 6), and may support a Kondo-like scattering mechanism. However, in addition to the magnetic and nonmagnetic Kondo-type scattering, the effect of two-dimensional weak localization (2DWL) leads the resistivity to show a $-\ln T$ dependence as well.[31–33] This behavior was previously observed, for instance, in a number of low-dimensional systems, such as $CuCl_2$, $CoCl_2$, $SbCl_5$, and also in graphite intercalation $MoCl_5$ compounds.[34,35] According to theories related to this effect, the weak localization phenomenon is an inherent interference effect common to any wave propagation in a disordered medium.[31,33,37] This effect occurs when the probability for the elastic scattering is much larger than that of the inelastic one. The occurrence of the 2DWL effect in $UCo_{0.5}Sb_2$ seems to be justified. First, the presence of numerous vacancies in the Co atom layers which are potential centers for the elastic scattering of charge carries increases the probability for such a kind of scattering. The observed value of the residual resistivity, being as large as 360 $\mu\Omega$ cm, is in agreement with this interpretation. Second, the possibility of the occurrence of the two dimensionality in $UCo_{0.5}Sb_2$ is relatively easy to understand owing to the layer type of crystal structure of this compound. Hence, the final expression for the resistivity in the ordered state for $J\perp c$ can then be expressed as follows:

$$\rho(T) = \rho_0 + \rho_{\mathrm{mag}} + C_{\mathrm{LT}}\ln T. \quad (6)$$

From the fitting data between temperatures 1.3–35 K, we have obtained the following parameters: ρ_0=360(1) $\mu\Omega$ cm, $A=6.5(3)\times10^{-3}$ $\mu\Omega$ cm K^{-2}, Δ=68(1) K, and $C_{\mathrm{LT}}=-0.78(1)$ $\mu\Omega$ cm K^{-1}. The result of the fits to Eq. (6) is illustrated as the solid line in the inset of Fig. 6.

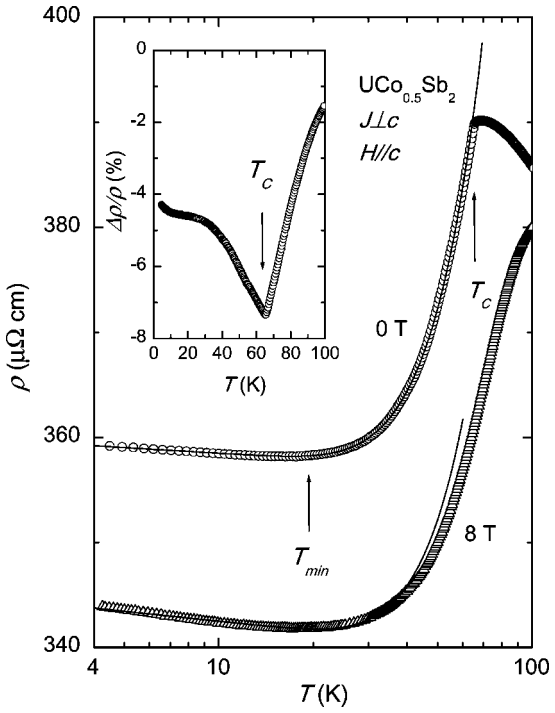

FIG. 7. Temperature dependence of the electrical resistivity measured at 0 and 8 T for J perpendicular to the c axis. The solid lines are fits to the experimental data. The inset shows the magnetoresistance as a function of temperature.

D. Magnetoresistance

The effect of an applied magnetic field on the resistivity can be seen in Fig. 7, where we compare the resistivity measured at a fixed field of 8 T with that of the zero field for $J\perp c$. The field was applied along the c axis, perpendicular to the current. One aspect we would like to emphasize here is the temperature dependence of the resistivity measured at 8 T at low temperatures. Since the $\rho(8\ \mathrm{T},T)$ curve below 40 K can be also well fitted with Eqs. (5) and (6) we conclude that the same scattering mechanism persists there as that in the zero-T resistivity, i.e., both the zero- and 8-T resistivities are governed mainly by both the spin-wave scattering and 2DWL effect and eventually in addition by a Kondo-like effect either conventional or non-magnetic. Furthermore, we found that the magnitude of the gap is considerably altered by the applied magnetic field. Keeping $A=6.5\times10^{-3}$ $\mu\Omega$ cm K^{-2} in the fit we obtain $C_{\mathrm{LT}}=-1.45$ $\mu\Omega$ cm K^{-1} and $\Delta(8\ \mathrm{T})=78(3)$ K. The change in the magnitude of Δ in the applied magnetic field is caused by an additional Zeeman-type contribution to the gap $\Delta(H)=\Delta(0)+g\mu_B\mu_0H$. For a field of 8 T the $g\mu_B\mu_0H$ contribution amounts to 4.3 K when we take g=0.8 in the case of the U^{4+} ion. The mechanism for a change in the C_{LT} value due to the magnetic field will be discussed below.

Magnetoresistance (MR) defined as $\Delta\rho/\rho=[\rho(T,B)-\rho(T,0)]/\rho(T,0)$, is shown as a function of temperature in the inset of Fig. 7. At 8 T the MR is negative over the investigated temperature range. The negative MR is passing through a sharp minimum around T_C, where it reaches a value $\Delta\rho/\rho=-7.5\%$. The observed effect is expected for the

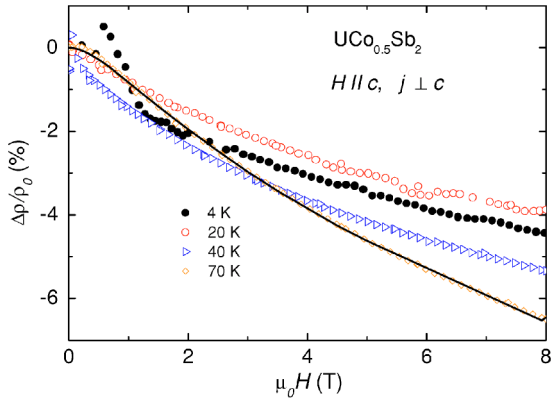

FIG. 8. Magnetoresistance measured at several temperatures as a function of the magnetic field. The solid line is a fit to the experimental data at 70 K.

MR due to damping of the critical fluctuations by the field.[36] The negative MR for $T > T_C$ may be interpreted as due to the suppression of the Kondo type and the existence of expanded critical fluctuations. As can be seen in Fig. 8, the shape of the $(\Delta\rho/\rho)(B)$ curve taken a little above T_C, e.g., at 70 K refers to the case where the latter mechanism becomes dominant in $UCo_{0.5}Sb_2$.

A remarkable feature is found for the MR at temperatures below 30 K, where the MR shows a weak temperature dependence, retaining an average value of about -4.5% up to this temperature. In order to clarify any mechanism responsible for this phenomenon, one needs to separate the total MR into partial magnetoresistances. For instance, in general we can distinguish some known contributions to the MR, such as the ordinary MR due to the orbital motion of the electrons in a magnetic field, contributions due to the anisotropic scattering, elastic scattering on defects and impurities, inelastic scattering on charge carriers, and finally scattering on local magnetic moments. However, by bearing in mind that the MR is a superposition of different contributions, its separation into each particular contribution is usually rather a sophisticated task and often not possible to be accomplished. Especially, we have no idea how to make such a separation in the MR being related with the anisotropic scattering. Nevertheless, we suppose that the contribution from the ordinary MR (Lorentz type) being always positive, may be negligible because our total MR is essentially negative. A presumption of a minor contribution from the Kondo-type effect one can accept as well. Based on the two-conduction-band periodic Anderson model, Chen *et al.*[38] obtained a negative magnetoresistance for a Kondo-hole disorder. However, it is well known that the field dependence of magnetoresistance for a Kondo system, in general, is scaled to the Kondo temperature T_K.[39] For $UCo_{0.5}Sb_2$, the MR data do not obey the scaling function $\Delta/\rho \sim f(H/H^*)$, where $H^*(T) = H^*(0) + k_B T/g\mu$ and $H^*(0) = k_B T_K/g\mu$. Thus, the description of the resistivity below 20 K in terms of a Kondo-type effect as the $\ln T$ dependence becomes unreliable.

As far as the magnetic scattering effect in the presence of a magnetic field is concerned, one has to put forward an argument that the magnetic scattering process is caused by several reasons. Similar to the way a magnetization process is governed by the domain effect, the orientation of magnetic moments and the change in the density of states is due to an applied field. Thus, to study the possible contributions to the MR due to the magnetic scattering on local spins, we will consider the relation between the MR and magnetization for each temperature measured. There have been several theoretical studies assuming an existence of the relationship between the magnetization and magnetoresistance. One of the models which is worth mentioning here is the effective exchange interaction model developed by Peski-Tinbergen and Dekker.[40] According to these authors, the relevant parameters V and J are taken into account, where V is the spin-independent electron scattering potential and J is the effective exchange interaction integral between the spin s of the conduction electrons and spin S of the local moments. The magnetoresistance is then given by the relation

$$\rho(H)/\rho(0) = 1 + aM(H,T)\tanh(g\mu_B H/2k_B T) - \frac{c^2 M(H,T)^2}{1 + aM(H,T)\tanh(g\mu_B H/2k_B T)}, \quad (7)$$

where constants a and c are dependent on the parameters V and J. In fact, this model has been used to explain the magnetoresistance behavior of systems showing a large magnetoresistance.[41,42] Other models are based either on the s-d indirect Hamiltonian or Kondo lattice Hamiltonian with the ferromagnetic-type coupling.[43,44] Both these latter models provide the relation

$$\rho(H)/\rho(0) = 1 + CM^2, \quad (8)$$

where C is a constant involving the saturation magnetization. To correlate the behavior of the MR and M, we have taken into account an isothermal magnetization for $H \| c$ axis and magnetoresistance trying to fit these data into the models mentioned above. However, we have obtained fits of poor quality for the magnetoresistance data collected below T_C. In turn, by using Eq. (7) a good fit could be attained for the data at 70 and 80 K, i.e., above T_C, where short-range ferromagnetic correlations still persist. The result of the fit for the data collected at 70 K is illustrated in Fig. 8.

The fact that we have not gotten a reliable relationship between the M and MR for $T < T_C$ may suggest that the magnetoresistance associated with the magnetization process does not give any important contribution to the total magnetoresistance. In order to simplify further analyses we will assume that at low temperatures, far below the Curie temperature T_C and magnon gap Δ, say below about 40 K, the contribution from the inelastic scattering process is significantly smaller than those from the elastic and magnetic scatterings, because the critical scattering as well as the electron-magnon process is expected to be no longer important at low temperatures. In consequence, the contribution to the MR from the scattering on the nonmagnetic centers in their atomic layers should play a dominant role at low temperatures.

As we have discussed above, one of the possible explanations for the occurrence of a $-\ln T$ dependence of the resistivity at low temperature is the 2DWL effect. This effect appears basically in disordered systems, where the propaga-

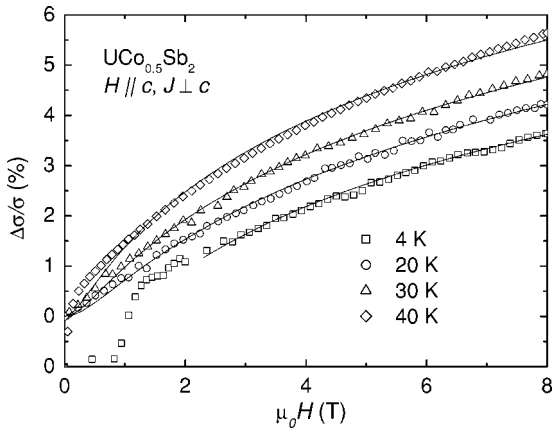

FIG. 9. Field dependence of the magnetoconductance of $UCo_{0.5}Sb_2$. The solid lines are fits to the experimental data.

tion wave of conduction electrons is believed to split into two waves interfering in the backscattering direction. A magnetic field introduces a magnetic phase shift and therefore suppresses the interference. Hence, it leads to the destruction of the localization effect and, in consequence, the magnetoresistance is expected to be negative.[33]

For a clarity of our analysis, we recall some important points of the weak localization theories for 2D system. In the case of the magnetic field applied perpendicular to a plane of 2D electronic systems, the conductance is given by[31,37,45,46]

$$\sigma(H,T) = \sigma(\infty) + \frac{e^2}{2\pi\hbar}\left[-\Psi\left(\frac{1}{2}+\frac{H_1}{H}\right)+\frac{3}{2}\Psi\left(\frac{1}{2}+\frac{H_2}{H}\right) - \frac{1}{2}\Psi\left(\frac{1}{2}+\frac{H_3}{H}\right)\right]. \quad (9)$$

In Eq. (9), $\sigma(\infty)$ is the conductance in the infinite magnetic field, ψ is digamma function, and H_1, H_2, and H_3 are defined by $H_1=H_0+H_{SO}+H_s$, $H_2=H_i+\frac{4}{3}H_{SO}+\frac{2}{3}H_s$, and $H_3=H_i+2H_s$. The quantities H_k with indexes $k=0$, SO, s, and i represent the characteristic fields associated with different scattering mechanisms, such as 0: elastic, i: inelastic, s: magnetic impurity, and SO: spin-orbit coupling. For $H=0$,

$$\sigma(0,T) = \sigma(\infty) + \frac{e^2}{2\pi\hbar}\frac{H_2^{3/2}}{H_1 H_3^{1/2}}$$

and therefore the magnetoconductance becomes

$$\frac{\sigma(H,T)-\sigma(0,T)}{\sigma(0)} = \frac{e^2}{2\sigma(0)\pi\hbar}\left[-\Psi\left(\frac{1}{2}+\frac{H_1}{H}\right)+\frac{3}{2}\Psi\left(\frac{1}{2}+\frac{H_2}{H}\right)-\frac{1}{2}\Psi\left(\frac{1}{2}+\frac{H_3}{H}\right)-\ln\left(\frac{H_2^{3/2}}{H_1 H_3^{1/2}}\right)\right]. \quad (10)$$

We have fitted Eq. (10) to the experimental data for $T \leqslant 50$ K, however, the fitting procedure was not good. This can be perceived in the fitting values of H_2 and H_3 of the order of fitting errors and which are practically undistinguished from each other. The reason for it is because of the large number of fitting parameters used. Also the contributions of the magnetic impurity scattering and spin-orbit coupling are suspected to be small. The assumption $H_s=H_{SO}=0$, $H_1=H_0$, and $H_2=H_3=H_i$, which was also made in some prior works,[45,47] seems to give a good fit to our experimental data. The results of the fits to Eq. (10) are marked by the solid lines in Fig. 9, and the rendered values for three parameters $e^2/2\sigma(0)\pi\hbar$, H_0, and H_i are listed in Table I. The values of the prefactor H_0 hold on the level of about 10 T for temperatures below 40 K, and they are much larger than those for the other H_i values. Since $H_k \sim 1/\tau_k$, we have the situation where $\tau_0 \ll \tau_i$ which provides the excellent conditions for the occurrence of the WL effect. We suppose that this mechanism is able to explain the enlargement of the coefficient C_{LT} at 8 T.

TABLE I. Parameters found by fitting of the experimental data utilizing Eq. (10).

T (K)	$\frac{e^2}{2\sigma(0)\pi\hbar}$(%)	$\mu_0 H_i$ (T)	$\mu_0 H_0$ (T)
4	2.78	0.21	10.5
20	2.09	0.29	10.7
30	2.99	0.22	9.7
40	2.88	0.16	10.9

E. Thermoelectric power

The temperature dependence of the thermoelectric power $S(T)$ measured along the two principal axes is shown in the form of the double logarithmic plot in Fig. 10. It is apparent that $S(T)$ of $UCo_{0.5}Sb_2$ is positive over the whole temperature range investigated and is indicative of a p type of material. We observe that the $S(T)$ curves show a highly anisotropic behavior, similar to the other physical properties studied here. With the heat flow Q applied along the c axis, the thermoelectric power $S_{\|}$ first decreases monotonically with decreasing temperature and near 100 K shows a broad

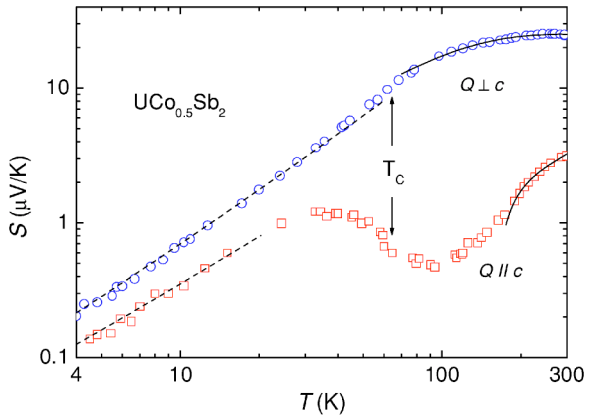

FIG. 10. Thermoelectric power in double logarithmic scales measured with the heat flow along the c axis and ab plane as a function of temperature. The dashed and solid lines are fits to the experimental data.

minimum. Below ~70 K, i.e., at temperatures close to T_C, $S_\parallel$ starts to increase reaching a maximum around 35 K. In contrast, the thermoelectric power $S_\perp$ with $Q \perp c$ axis does not show a minimum and has at room temperature a relatively large value of 25 μV/K, i.e., several times larger than the value of 3.4 μV/K yielded by the parallel component $S_\parallel$. The former first decreases slowly with decreasing temperature and below $T \approx 100$ K a systematic drop in $S_\perp(T)$ is observed.

A rather unexpected feature found in the $S(T)$ curves is imperceptible contribution of the phonon drag. Generally, in the thermoelectric power of a magnetic compound, apart from the electron diffusion and magnon-drag contributions, we should usually observe a phonon-drag contribution, which at low temperatures follows the power dependence T^3, as the lattice specific heat does. In fact, both the $S_\parallel(T)$ and $S_\perp(T)$ curves in the temperature range 4–20 K take the form

$$S = \alpha T + \beta T^{3/2} \tag{11}$$

which is illustrated as the dashed lines in Fig. 10. In Eq. (11) the first and second term represent the diffusion and magnon drag contributions to the total thermopower, respectively. The observation of the $T^{3/2}$ dependence of $S(T)$ supports our interpretation in terms of the spin-wave theory. On the other hand, the magnon-drag process is often reflected by the occurrence of a maximum in $S(T)$, usually between $T_C/10 < T < T_C/5$,[48] which in fact is not detected in our data. Also the fact of the lack of a distinct anomaly near T_C in the $S_\perp(T)$ curve leads us to suspect that the magnon-drag contribution to S is of minor importance compared with the other contributions, namely, those originating from the magnon-magnon and magnon-phonon scattering, discussed, for example, many years ago by Morkowski.[49] Consequently, the observed changes in both $S_\perp(T)$ and $S_\parallel(T)$ in the vicinity of T_C may be interpreted in terms of changes taking place in the structure of the density of states at the Fermi level E_F corresponding to the diffusion thermopower. This mechanism, in accordance to the Mott's formula may be presented as[50]

$$S = \frac{\pi^2 k_B}{3|e|} k_B T \left[\frac{\partial \ln \sigma}{\partial \epsilon} \right]_{\epsilon = E_F} = \frac{\pi^2 k_B}{3|e|} k_B T \times \left[\frac{\partial \ln N(E_F)}{\partial \epsilon} + \frac{\partial \ln \tau}{\partial \epsilon} \right]_{\epsilon = E_F}. \tag{12}$$

Accordingly, S depends not only on the energy derivative of the relaxation time of the conduction electrons $\partial\tau/\partial\epsilon$, but also on a derivative of the density of states $N(E_F)$. This means that S is very sensitive to the change in the electronic band structure near E_F, which is usually accompanied by a magnetic phase transition.

Next we discuss a highly anisotropic behavior observed in the temperature dependence of the thermopower of $UCo_{0.5}Sb_2$. First of all, the large values of $S_\perp$ observed in the paramagnetic state, compared to those of $S_\parallel$, suggest a two-dimensional motion of the carriers. Within the *ab* plane, where the magnetic uranium moments tend to align parallel, the carriers become scattered on the localized magnetic moments much more effectively than along the *c* axis. Moreover, the relaxation time of conduction electrons is altered very much due to the presence of vacancies in the Co layers. This may lead to a larger value of S measured in the configuration $Q \| ab$ plane. On the other hand, any anisotropy in the thermopower should be correlated to an anisotropic structure of the Fermi surface. Unfortunately, no information on the Fermi surface is available at the moment.

Finally, we may also interpret the high-temperature $S(T)$ behavior with the help of a phenomenological model for a Kondo lattice.[51] The presence of the Kondo effect in the temperature dependence of the resistivity found in the paramagnetic state justifies the application of a Kondo-type model for the $S(T)$ dependencies. According to Freimuth's model,[51] which was used by Garde and Ray[52] in the case of Ce-based compounds, a high-temperature value of the thermopower of an *f*-electron system due to the scattering between the conduction electrons of the broad *s-d* bands and the *f* electrons of the narrow shaped Lorentzian bands can be described using the following phenomenological formula:

$$S(T) = \alpha T + \frac{C T T_0}{T_0^2 + W^2}, \tag{13}$$

where

$$W = T_f \exp(-T_f/T).$$

C, T_0, and T_f are the characteristic constants, determining the magnetic scattering process. It appears that T_f is the temperature-dependent parameter, which sets the width W of the *f* band, while T_0 represents the position of the *f* band with respect to the Fermi level, i.e., $k_B T_0 = |E_F - E_f|$. Though the fitting of Eq. (13) to the experimental data, shown in Fig. 10 as the solid lines, may have only a qualitative meaning, it reflects the importance of the results of our calculations. They are as follows. (i) It has been possible to reproduce in the paramagnetic state the temperature dependence of the $S(T)$ dependencies. (ii) The temperature $T_f = 194(10)$ K for $S_\perp$, comparable to the position of a broad maximum observed in the $S_\perp(T)$ curve, is almost three times smaller than that for $S_\parallel$, $T_f = 680(30)$ K. (iii) A narrow *f* band in the *ab* plane is characterized by the position of $T_0 = 125(14)$ K. In contrast, a broader *f* band is formed along the *c* axis with $T_0 = -8(3)$ K. This may suggest that the hybridization between the 5*f* electrons and conduction electrons along the *c* axis is much stronger than that in the *ab* plane.

IV. SUMMARY

We have measured the magnetization, specific heat, electrical resistivity, magnetoresistance, and thermoelectric power of single crystals $UCo_{0.5}Sb_2$. The observed anomalies are consistent with the onset of ferromagnetic order below $T_C = 64.5(2)$ K. A scaling analysis of the isothermal magnetization provided a precise value of the Curie temperature and the magnetization critical exponents. At temperatures below about $T_C/2$, two types of magnetic excitations are observed; the spin-wave and Stoner-type excitations. We have estimated the spin-wave stiffness coefficient D. A relative large D/T_C ratio found suggests the presence of strong fer-

romagnetic interactions between the nearest located uranium magnetic moments. The most exciting finding in our work is the observation of the 2DWL effect in $UCo_{0.5}Sb_2$. This effect, together with the electron magnon scattering one, is thought to be the main mechanism governing the temperature dependence of the resistivity in the ordered state. The latter mechanism can be described by taking into account a gap Δ in the magnon spectrum, which is slightly altered by the applied magnetic field. The change in the magnitude of the gap is interpreted as an additional Zeeman term which should be added to the gap determined at zero field. Negative magnetoresistance is observed over a wide temperature range below 150 K. The behavior of the magnetoresistance taken at temperatures far below T_C is consistent with the interpretation in terms of the elastic scattering in a 2D system with the weak localization effect. We have ascribed the effect of the magnetic field on the magnetoresistance around T_C as being due to the suppression of the critical scattering fluctuations. In the paramagnetic state, the resistivity of $UCo_{0.5}Sb_2$ with $J \perp c$ axis is characterized by a $-\ln T$ dependence which is indicative of the Kondo-type behavior. Based on spin-wave theory, we were able to account for the $T^{3/2}$ dependence observed in the thermoelectric power of $UCo_{0.5}Sb_2$ at temperatures below $T_C/2$. The applied here phenomenological Kondo lattice model could give an adequate description for the temperature dependencies of $S(T)$ at high temperatures. As to our knowledge, $UCo_{0.5}Sb_2$ is the first ternary uranium compound showing the characteristics of the two-dimensional weak localization effect. We believe that in conjunction with a Kondo-like manner, a strong ferromagnet $UCo_{0.5}Sb_2$ appears to be an interesting enough compound for further investigations, especially with respect to its low dimensionality.

ACKNOWLEDGMENTS

The authors acknowledge the financial support from a KBN Grant No. 2 PO3B 109 24 and thank Mr. R. Gorzelniak for his assistance with the magnetic measurements.

[1] N. K. Sato, N. Aso, K. Miyake, R. Shiina, P. Thalmeier, G. Varelogiannis, C. Geibel, F. Steglich, P. Fulde, and T. Komatsubara, Nature (London) **410**, 340 (2001).
[2] G. Zwicknagl, A. Yaresko, and P. Fulde, Phys. Rev. B **65**, 081103(R) (2002); G. Zwicknagl, A. Yaresko, and P. Fulde, *ibid.* **68**, 052508 (2003).
[3] D. Kaczorowski, R. Kruk, J. P. Sanchez, B. Malaman, and F. Wastin, Phys. Rev. B **58**, 9227 (1998).
[4] M. Brylak, M. H. Mller, and W. Jetschko, J. Solid State Chem. **115**, 305 (1995).
[5] Z. Bukowski, V. H. Tran, J. Stępień-Damm, and R. Troć, J. Solid State Chem. **177**, 3934 (2004).
[6] Z. Bukowski, D. Kaczorowski, J. Stępień-Damm, D. Badurski, and R. Troć, Intermetallics **12**, 1381 (2004).
[7] J. C. Slater, Phys. Rev. **52**, 198 (1937).
[8] C. Herring and C. Kittel, Phys. Rev. **81**, 869 (1951).
[9] E. D. Thompson, E. P. Wohlfarth, and A. C. Bryan, Proc. Phys. Soc. London **83**, 59 (1964).
[10] A. T. Aldred, Phys. Rev. B **11**, 2597 (1975).
[11] E. Babic, Z. Marohnic, and E. P. Wohlfarth, Phys. Lett. **95A**, 335 (1983).
[12] Y. Endoh and K. Hirota, J. Phys. Soc. Jpn. **66**, 2264 (1997).
[13] L. Paolasini, G. H. Lander, S. M. Shapiro, R. Caciuffo, B. Lebech, L.-P. Regnault, B. Roessli, and J.-M. Fournier, Phys. Rev. B **54**, 7222 (1996).
[14] S. K. Ma, *Modern Theory of Critical Phenomena* (W. A. Benjamin, New York, 1976).
[15] M. E. Fisher and J. S. Langer, Phys. Rev. Lett. **20**, 665 (1968).
[16] I. Mannari, Prog. Theor. Phys. **22**, 335 (1959).
[17] I. A. Campbell and A. Fert, in *Ferromagnetic Materials*, edited by E. P. Wohlfarth (North-Holland, Amsterdam, 1982), Vol. 3, p. 747.
[18] N. H. Anderson and H. Smith, Phys. Rev. B **19**, 384 (1979).
[19] A. de la Torre Lopez, P. Visani, Y. Dalichaouch, W. Lee, and M. B. Maple, Physica B **179**, 208 (1992)
[20] A. M. Strydom, P. de V. du Plessis, and V. H. Tran, Solid State Commun. **112**, 391 (1999).
[21] V. H. Tran, A. Hoser, and M. Hofmann, J. Phys.: Condens. Matter **12**, 1029 (2000).
[22] Y. Onuki and T. Komatsubara, J. Magn. Magn. Mater. **63-64**, 281 (1987).
[23] J. M. Lawrence, T. Graf, M. F. Hundley, D. Mandrus, J. D. Thompson, A. Lacerda, M. S. Torikachvili, J. L. Sarrao, and Z. Fisk, Phys. Rev. B **53**, 12 559 (1996).
[24] C. Mazumdar, R. Nagarajan, C. Godart, L. C. Gupta, B. D. Padalia, and R. Vijayaraghavan, J. Appl. Phys. **79**, 6347 (1996).
[25] R. Sollie and P. Schlottmann, J. Appl. Phys. **69**, 5478 (1991); **70**, 5803 (1991); P. Schlottmann, *ibid.* **75**, 7045 (1994); P. Schlottmann, Phys. Rev. B **46**, 998 (1992); Physica B **206-207**, 816 (1995).
[26] S. Doniach and P. Fazekas, Philos. Mag. B **65**, 1171 (1992).
[27] S. Wermbter, K. Sabel, and G. Czycholl, Phys. Rev. B **53**, 2528 (1996).
[28] Z. Henkie, A. Wojakowski, R. Wawryk, T. Cichorek, and F. Steglich, Acta Phys. Pol. B **34**, 1323 (2003).
[29] T. Cichorek, H. Aoki, J. Custers, Ph. Gegenwart, F. Steglich, Z. Henkie, E. D. Bauer, and M. B. Maple, Phys. Rev. B **68**, 144411 (2003).
[30] D. L. Cox and A. Zawadowski, Adv. Phys. **47**, 599 (1998).
[31] S. Hikami, A. I. Larkin, and Y. Nagaoka, Prog. Theor. Phys. **63**, 707 (1980).
[32] B. L. Altshuler, A. G. Aronow, and P. A. Lee, Phys. Rev. Lett. **44**, 1288 (1980).
[33] P. A. Lee and T. V. Ramakrishnan, Rev. Mod. Phys. **57**, 287 (1985), and references therein.
[34] L. Piraux, J.-P. Issi, J.-P. Michenaud, E. McRae, and J. F. Mareche, Solid State Commun. **56**, 567 (1985); L. Piraux, V. Bayot, J.-P. Michenaud, J.-P. Issi, J. F. Mareche, and E. McRae, Solid State Commun. **59**, 711 (1986); L. Piraux, V. Bayot, X. Gonze, J.-P. Michenaud, and J.-P. Issi, Phys. Rev. B **36**, 9045

(1987).
[35] M. Suzuki, C. Lee, I. S. Suzuki, K. Matsubara, and K. Sugihara, Phys. Rev. B **54**, 17 128 (1996).
[36] H. Yamada and S. Takada, J. Phys. Soc. Jpn. **34**, 51 (1973); Prog. Theor. Phys. **49**, 1401 (1973).
[37] G. Bergmann, Phys. Rev. B **28**, 2914 (1983); Phys. Rep. **107**, 1 (1984).
[38] C. Chen, Z. Z. Li, and W. Xu, J. Phys.: Condens. Matter **5**, 95 (1993); C. Chen and Z. Z. Li, *ibid.* **6**, 2957 (1994) .
[39] P. Schlottmann, Z. Phys. B: Condens. Matter **49**, 109 (1982); **51**, 223 (1983); **51**, 49 (1983).
[40] T. Van Peski-Tinbergen and A. J. Dekker, Physica (Amsterdam) (Amsterdam) **29**, 917 (1963).
[41] J. Q. Wang, P. Xiong, and G. Xiao, Phys. Rev. B **47**, 8341 (1993).
[42] V. H. Tran and R. Troć, Phys. Rev. B **57**, 11 592 (1998).
[43] K. Kubo and N. Ohata, J. Phys. Soc. Jpn. **33**, 21 (1972).
[44] N. Fukukawa, J. Phys. Soc. Jpn. **63**, 3214 (1994).
[45] V. Bayot, L. Piraux, J.-P. Michenaud, and J.-P. Issi, Phys. Rev. B **40**, 3514 (1989); **41**, 11 770 (1990).
[46] R. Rosenbaum, Phys. Rev. B **32**, 2190 (1985).
[47] Y. Wang and J. J. Santiago-Aviles, J. Appl. Phys. **94**, 1721 (2003).
[48] F. J. Blatt, P. A. Schroeder, and C. L. Foiles, *Thermoelectric Power of Metals* (Plenum Press, New York, 1976).
[49] A. Morkowski, Phys. Lett. **21**, 146 (1966).
[50] J. M. Ziman, *Electrons and Phonons* (Oxford University Press, Oxford, 1960).
[51] A. Freimuth, J. Magn. Magn. Mater. **68**, 28 (1987).
[52] C. S. Garde and J. Ray, Phys. Rev. B **51**, 2960 (1995).